

A NOVEL MINEFIELD DETECTION APPROACH BASED ON MORPHOLOGICAL DIVERSITY

Yuming Wang^{*}, Qian Song, Tian Jin, Xiaotao Huang, and Hanhua Zhang

School of Electronic Science and Engineering, National University of Defense Technology, Changsha, Hunan 410073, China

Abstract—Battlefield surveillance is a common application of synthetic aperture radar (SAR), in which minefield detection is a challenging task. In this paper, a novel minefield detection approach is proposed via the morphological diversities between targets and background. Firstly, SAR image speckle is suppressed effectively by total variation, and targets edges are preserved well. Secondly, a nonlinear transform is introduced to map the special distributed targets, e.g., landmines, into spot targets. Lastly, the modification of morphological component analysis is adopted to improve the signal-to-clutter ratio and separate the spot targets from image. The performance of the proposed approach is validated by using the data acquired over an airship mounted SAR system.

1. INTRODUCTION

Nowadays, there is an increasing interest in remote sensing applications from low-altitude platform. One of the most encouraged applications is minefield surveillance by airship. Synthetic aperture radar (SAR) is able to provide a powerful surveillance capability, allowing the observation of broad expanses, independently from weather conditions, so much during the day as during the night [1]. Ultra-wideband (UWB) SAR, operating in low frequency, can penetrate the ground surface, so minefield detection via UWB SAR is one of the highlights of research [2–4].

But the counterpart is that the minefield detection in SAR images, affected by speckle, is quite troublesome. Ground clutters are another reason for detection performance depreciation. Generally, there exist

Received 15 November 2012, Accepted 9 January 2013, Scheduled 18 January 2013

* Corresponding author: Yuming Wang (yumingwang_1985@yahoo.com.cn).

lots of trees, stones and bumps, etc., in surveillance scene, which have strong reflections in radar system. So those objects lead to a lot of false alarms in detection images when the processing of detecting only relies on the images gray, such as the local constant false alarm rate (CFAR) detector and RX anomaly detector [5,6]. In order to reduce false alarms, other features of landmine should be extracted, e.g., morphological features.

When the resolution of SAR image is high enough, landmines are shown as round patch, which can be considered as distributed targets. Besides, landmines which are laid by machine in one terrain have the same materials, and they exhibit similar geometric shape. This paper intends to establish a framework of detecting landmines in minefield using morphological features.

With the development of sparse representation theory [4,7], the algorithm of morphological component analysis (MCA) is adopted to realize the image decomposition, image inpainting, and blind source separation [8–10]. In this paper, we use the modification of MCA to separate landmines from SAR images. The fundament of MCA is the different sparsity of texture or background in specific dictionary, such as curvelet [11] and discrete cosine transformation (DCT) [12]. It is well known that curvelet can express linear abrupt targets sparsely while DCT is sensitive to abrupt spot targets. MCA is often adopted to deal with optical images, but it is hardly to be seen in SAR images processing. Since SAR images have high resolution, many targets in them manifest block structure, and their morphological edges change slowly. So MCA separates distributed targets from SAR images difficultly. Aimed at this problem, this paper makes use of a morphological map to transform target into a small spot, and then it separates the spot from image via MCA with components constraint (MCACC). Extended fractal is effective in analyzing distributed targets, it has been widely used for features extraction and target detection [13,14]. Extended fractal is a deviation of the multiscale Hurst parameter used to quantize the roughness of a target at various scales. Since extended fractal is actually sensitive to both the size and intensity of the target. Through a judicious selection for the parameter values of the computational algorithm, we can take advantage of it to map landmine imagery into a spot in the new feature image.

We design a minefield detection approach which connects extended fractal and MCACC, it can achieve high detection rate and keep a low false alarms rate. Besides, in order to reduce the affection of speckle, the total variation (TV) algorithm is adopted at first [15,16]. The remainder of this paper is organized as follows. In Section 2, we

give a brief description on the speckle suppression. In Section 3, the morphological characteristics of landmine are analyzed, and the theory of MCA is introduced. In Section 4, the proposed minefield detection approach is discussed in details. Section 5 gives the experimental results. Finally, the conclusions are drawn in Section 6.

2. SPECKLE SUPPRESSION

In SAR image, speckle is generated when it receives random interference of electromagnetic waves reflected by many principal scatterers, and it makes the images hard to interpret. The classical algorithms of speckle suppression contain Lee filter, Kuan filter, and so on [17, 18]. They expect to preserve features and retain image texture as well as edges. But most of their capacities are founded on the accuracy of statistical models which are established for speckle [19]. As a result, good performances will be hardly achieved when those models are mismatched.

It has been proved that TV is an effective tool for image speckle suppression, which is proposed by Rudin et al. [15]. We assume that $s(r, x)$ is a SAR image, where (r, x) is the position of a point in it. The image \hat{s} after denoising can be obtained by the following formula,

$$\min_f \int_{\Omega} |\nabla \hat{s}| dr dx \quad s.t. \quad \frac{1}{2} \int_{\Omega} (s - \hat{s})^2 dr dx \leq \sigma^2 \quad (1)$$

where ∇ denotes gradient, and Ω is a bounded domain, $r, x \in \Omega$. In order to solve this optimum problem, Equation (1) is expressed as

$$\hat{s} = \arg \min_{\hat{s}} \left\{ \int_{\Omega} |\nabla \hat{s}| dr dx + \frac{\lambda_1}{2} \int_{\Omega} (s - \hat{s})^2 dr dx \right\} \quad (2)$$

where $\lambda_1 \geq 0$ is Lagrange multiplier. At the minimum point, the derivative of calculus equals zero. So the derivative of Equation (2) is written as

$$\nabla \cdot \left(\frac{\nabla \hat{s}}{|\nabla \hat{s}|} \right) + \lambda_1 (s - \hat{s}) = 0 \quad (3)$$

To solve the Equation (3), we use the steepest descent method which is proposed in [15]. Fig. 1(a) gives an original SAR image which is acquired by Airship-Mounted UWB SAR (AMUSAR) [20]. In this sense, there are 13 antitank landmines which marked by the dashed boxes. Fig. 1(b) shows the denoising image, and the speckle is suppressed via TV. The number of iteration for solving Equation (3) is 20, and the value of Ω equals the image size (950×550 pixels). By comparison with the images before and after TV, we know that the TV algorithm can smooth image effectively while it remains the target edges.

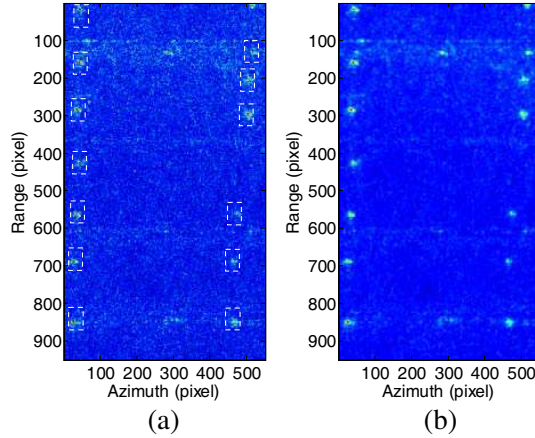


Figure 1. The results of speckle suppression. (a) Original SAR image containing 13 landmines marked by the dashed boxes; (b) the speckle suppression image via TV.

3. ANALYSIS OF LANDMINE MORPHOLOGICAL CHARACTERISTICS

In this section, the morphological characteristics of landmines and the principle of MCA are analyzed. MCA is capable of extracting different targets via their morphological diversities in images, so it can be applied for landmine detection since the geometric shape of landmines are consistent. The core of MCA is that different targets will be sparsely represented by different dictionaries, and the coefficients corresponded these dictionaries can be acquired by fast transformation. Curvelet and DCT are often adopted in MCA. In order to detect landmine, we will discuss the sparsity of landmines decomposition in curvelet and DCT dictionaries.

3.1. Morphological Component Analysis

MCA in this paper can be considered as a process of target separation, it is a promotion of sparse representation. \hat{s} is a linear combination of basic atoms as follows:

$$\hat{s} = \sum_{n=1}^N c_n d_n = D\mathbf{c} \quad (4)$$

where D is the dictionary and d_n is the atoms of D . $n(1 \leq n \leq N)$ is variable and N is the number of atoms. \mathbf{c} is the coefficients vector, $\mathbf{c} = [c_1, c_2, \dots, c_N]$. If the number of nonzero values in \mathbf{c} is small, we consider that \hat{s} is sparse in D .

Image sparse representation can be considered as a process of seeking the minimum number of nonzero values in \mathbf{c} . In order to simplify the solving difficulty, the optimization problem can be written as

$$\min_{\mathbf{c}} \|\mathbf{c}\|_1 \quad s.t. \quad \hat{s} = D\mathbf{c} \tag{5}$$

Basis Pursuit (BP) method [21, 22] is often adopted for solving Equation (5). But BP is computationally expensive. So reducing calculation is a research emphasis for improving this method. MCA is an alternative of BP method, and it can operate with little time and memory, because it has specific dictionaries. The derivation of MCA will be shown as follows.

Assuming that image \hat{s} is a linear combination of components, $\hat{s} = \sum_{m=1}^M s_m$, where s_m represents a different morphological component, and M is the number of components. D consists of sub-dictionaries D_m , $m = 1, \dots, M$, which has fast transformation T_k . Equation (4) can be written as

$$\hat{s} = \sum_m D_m \mathbf{c}^m \tag{6}$$

where \mathbf{c}^m is the vector of coefficients for D_m . In order to seek the sparsest representation over their overcomplete dictionaries containing all D_m , the following equation needs to be solved.

$$\{\tilde{\mathbf{c}}^1, \dots, \tilde{\mathbf{c}}^M\} = \arg \min_{\{\mathbf{c}^1, \dots, \mathbf{c}^M\}} \sum_{m=1}^M \|\mathbf{c}^m\|_1 \quad s.t. \quad \hat{s} = \sum_m D_m \mathbf{c}^m \tag{7}$$

To reduce the complexity of solving this optimization problem, MCA reformulates the problem of finding $\{\tilde{\mathbf{c}}^1, \dots, \tilde{\mathbf{c}}^M\}$ in getting s_m ($1 \leq m \leq M$). Since $\mathbf{c}^m = T_m s_m$, and Lagrange multiplier λ_2 is introduced, then the optimization function is written as

$$\{\tilde{s}_1, \dots, \tilde{s}_M\} = \arg \min_{\{s_1, \dots, s_M\}} \sum_{m=1}^M \|T_m s_m\|_1 + \lambda \left\| \hat{s} - \sum_{m=1}^M s_m \right\|_2^2 \tag{8}$$

where $\hat{s} - \sum_{m=1}^M s_m$ is the residual component. It expresses the part which cannot be represented sparsely by any D_m .

3.2. The Sparsity Analysis of Landmine Decomposition in Curvelet and DCT

Since curvelet and DCT can sparsely represent abrupt line and abnormal spot respectively, both of them are important dictionaries

in MCA. In this paper, we intend to take advantage of MCA to detect landmines. So the sparse characteristics of landmine decomposition in curvelet and DCT will be discussed. Brief descriptions of curvelet and DCT are given in the following context, and then simulation results about distributed targets are analyzed.

The curvelet is developed as a solution to the weakness of the wavelet in sparsely representing linear targets. Candes et al. have extended their work providing the second generation curvelet transform, which is a frequency analysis for each sub-band being divided in the frequency domain [11]. The lower frequency, the smaller bandwidth of the sub-band is. For each sub-band, this is divided further into several regions with different polar angles. So curvelet can take the form of basic elements which exhibit high directional sensitivity and are highly anisotropic. Curvelet has had an important success in images processing applications like denoising, texture analysis, and so on.

DCT is an effective transform which is widely used to compress images. Lots of researches have also been done in the realm of facial recognition. They use DCT to transform the image into a feature space which can then be used by an algorithm to classify the image. DCT coefficients may be manipulated for acquiring the low frequency information or high frequency information. The DCT formula of an image (size: $I \times J$) can be written as

$$\begin{cases} \hat{S}_{kl} = \sqrt{\frac{2}{I}} \sqrt{\frac{2}{J}} \sum_{i=0}^{I-1} \sum_{j=0}^{J-1} \hat{s}(i, j) \cos \left[\frac{(2i+1)k\pi}{2I} \right] \cos \left[\frac{(2j+1)l\pi}{2J} \right] \\ \hat{s}(i, j) = \sqrt{\frac{2}{I}} \sqrt{\frac{2}{J}} \sum_{k=0}^{I-1} \sum_{l=0}^{J-1} \hat{S}_{kl} \cos \left[\frac{(2i+1)k\pi}{2I} \right] \cos \left[\frac{(2j+1)l\pi}{2J} \right] \end{cases} \quad (9)$$

where $i, k = 0, 1, \dots, I-1$; $j, l = 0, 1, \dots, J-1$.

To analyze the sparse characteristics of landmine, we simulate three round targets, including two distributed targets and one small spot target. As shown in Fig. 2(a), the shape of left target is close to landmine image expressed in real SAR image, and the others targets are used for comparison. Fig. 2(b) gives the reconstruction image using the curvelet coefficients at the first level of high frequency. We can see that these round targets edges are manifested clearly, but other parts of them cannot be expressed whatever their radiuses are small or big. Fig. 2(c) shows the reconstruction image using high frequency coefficients after DCT. It is shown that the centers of the left and middle targets are discarded. However, the smallest target has almost been reconstructed completely. It suggests that we can map the

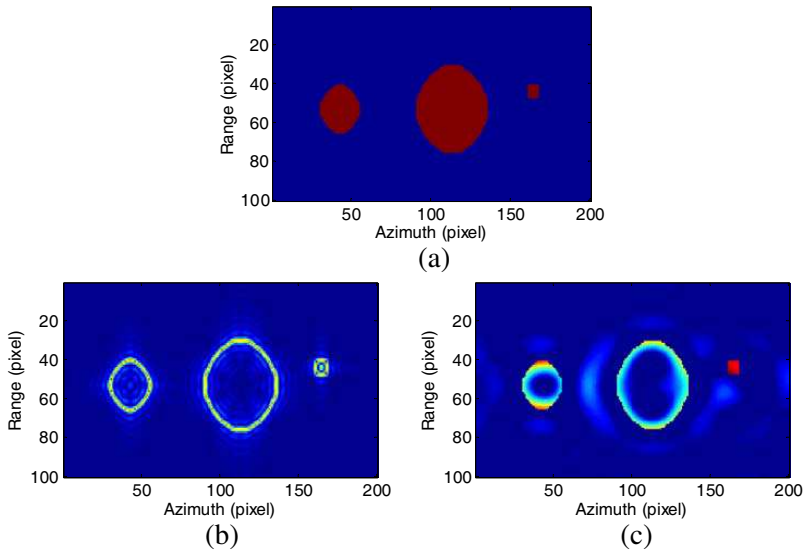


Figure 2. The results of simulation. (a) Original simulation image containing three round targets with radiuses being 12, 21, 3 respectively; (b) the reconstruction image via the curvelet coefficients at the first level of high frequency; (c) the reconstruction image via high frequency coefficients after DCT.

landmine into a small spot so as to separate it from image via DCT component.

4. MINEFIELD DETECTION APPROACH BASED ON MORPHOLOGICAL DIVERSITY

4.1. The Scheme of Minefield Detection Approach

As shown in Fig. 3, the approach of minefield detection consists of four steps. In order to reduce the affection of speckle and acquire accurate features, TV algorithm is adopted at the first step. According to the simulation results of Section 3.2, landmine can be sparsely represented neither by curvelet nor DCT. We need to design a function that maps the landmine into a spot target, which can be sparsely decomposed in DCT. So the second step of this scheme is nonlinear mapping. Extended fractal (EF) can extract the distributed characteristic, so we use it to form a strong spot by adjusting its window. At the third step, we want to take advantage of the MCA to separate the spot target from image, and then the landmine will be mainly contained in

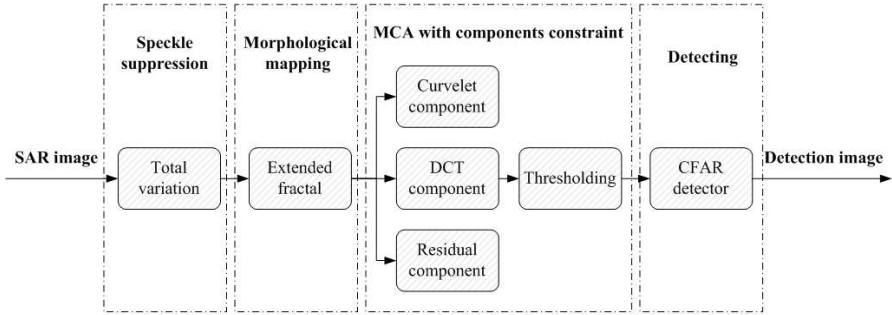


Figure 3. The scheme of minefield detection approach.

the DCT component. In the fourth step, CFAR detector is used to detect landmine, it can achieve a good performance when image has high local signal-to-clutter ratio (SCR).

Since MCA uses specific dictionaries which solving coefficients have fast transformation, it can reduce the time and memory of computation effectively. But it often adds the constraint on the components for noise suppression, and that cannot improve the speed of computation further. We intend to modify the constraint so as to make MCA to reach faster and convergent. Through analyzing the processing of MCA, we can conclude that the computing time of MCA mainly cost in cyclic iteration. So the effectively modification for MCA is to reduce the number of iteration.

Aiming at the above phenomenon, to reduce the number of iteration for solving Equation (8) and acquire good performance of sparse representation, the MCACC whose components are restricted is proposed. This paper restricts the landmine component s_t with the following formula

$$s_t^{i+1} = \begin{cases} s_t^i, & s_t^i \geq \text{mean}(s_t^i) + \mu \times \text{std}(s_t^i); \\ 0, & s_t^i < \text{mean}(s_t^i) + \mu \times \text{std}(s_t^i). \end{cases} \quad (10)$$

where i denotes the iterative number. $\text{mean}(\cdot)$ indicates the average value of samples, $\text{std}(\cdot)$ expresses the standard deviation of samples. μ is the weighting coefficient to control the convergence rate of iteration, and it equals to 2 in generally. According to Equation (10), components are segmented by threshold, and the expected values are preserved and the others are set to be zeros. That is, a constraint with target sparsity has been added on MCA components, and this can accelerate the convergence of iteration.

In terms of the process for minefield detection in Fig. 3, we

can know that the SCR increases step by step: (1) The TV can suppress the speckle effectively; (2) The EF also enhances the landmine intensity; (3) The extraction of landmine component using MCACC discards clutters and noise too. So the detection can achieve a good performance.

4.2. Extended Fractal Mapping

As given in Section 3.2, the landmine cannot be sparsely represented by both curvelet and DCT. So we intend to design a morphological mapping that makes the distributed target (landmine) into small spot

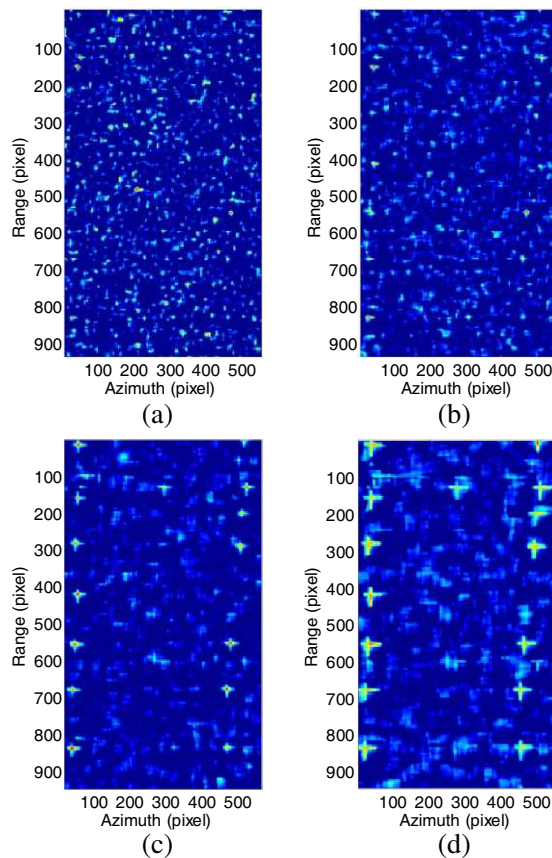


Figure 4. The mapping images via EF with different window sizes and lags. (a) $W_1 = 13$, $W_2 = 13$, $\Delta = 6$; (b) $W_1 = 17$, $W_2 = 17$, $\Delta = 8$; (c) $W_1 = 25$, $W_2 = 25$, $\Delta = 12$; (d) $W_1 = 33$, $W_2 = 33$, $\Delta = 16$.

which can be separated from image.

The feature of EF can express the morphological characteristic of target [13, 14]; we make use of it to map the landmine into spot target. In order to give the formula of computing EF, we define e_r^Δ , e_x^Δ firstly.

$$\begin{cases} e_r^\Delta(r, x) = \sum_{\alpha=1}^{W_1} \sum_{\beta=1}^{W_2} |\hat{s}(r + \Delta + \alpha, x + \beta) - \hat{s}(r - \Delta + \alpha, x + \beta)|^2 \\ e_x^\Delta(r, x) = \sum_{\alpha=1}^{W_1} \sum_{\beta=1}^{W_2} |\hat{s}(r + \alpha, x + \Delta + \beta) - \hat{s}(r + \alpha, x - \Delta + \beta)|^2 \end{cases} \quad (11)$$

where Δ is smallest lag, W_1 and W_2 are the size of slide windows in direction r and x , respectively. So the EF formula in these directions can be written as

$$\begin{cases} E_r(r, x) = \frac{1}{2} \log_2 \left(\frac{e_r^\Delta(r, x)}{e_r^{2\Delta}(r, x)} \right), \\ E_x(r, x) = \frac{1}{2} \log_2 \left(\frac{e_x^\Delta(r, x)}{e_x^{2\Delta}(r, x)} \right). \end{cases} \quad (12)$$

The EF feature E_{rx} used in this paper is the mean of E_r and E_x , which is expressed as

$$E_{rx} = \frac{E_r + E_x}{2} \quad (13)$$

In terms of Equations (11), (12) and (13), we can know that the EF feature is sensitive to the size of targets. So, it is possible to choose window sizes and lags for the EF extraction so that the mapping peaks out for landmine images. Fig. 4 is the processing result of Fig. 1(b), which gives the mapping images via EF with different



Figure 5. The AMUSAR system.

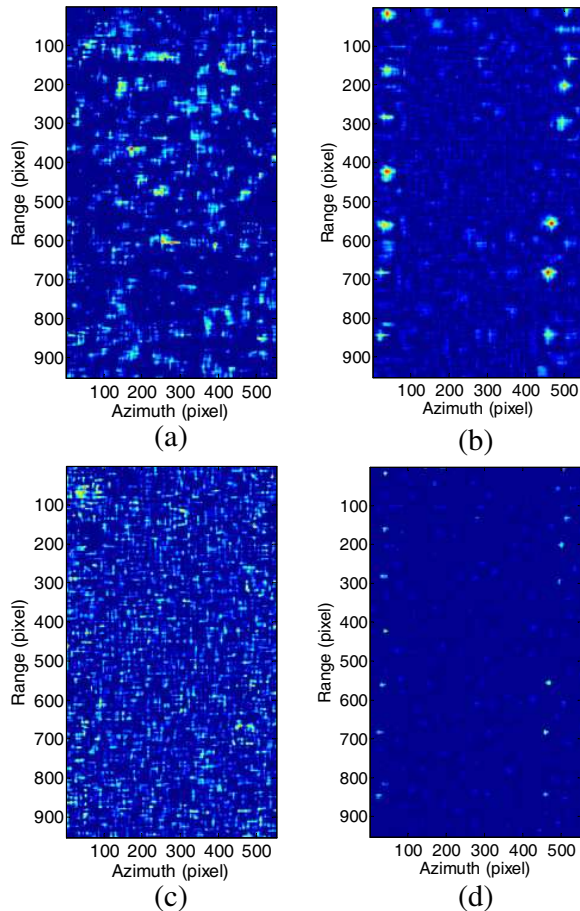


Figure 6. The processing results using modification algorithm of MCA. (a) Curvelet component; (b) DCT component; (c) the residual after discarding the components of curvelet and DCT; (d) the detection image of (b) via CFAR detector whose parameter of false alarms rate is 10^{-3} .

window sizes and lags. From Fig. 4(c), we can see that landmines will be mapped into strong spots with weak clutters when the window sizes are close to landmines sizes. As shown in Figs. 4(a) and 4(b), there exist many strong spots of clutters in the mapping images when the window sizes are smaller than landmines sizes. But when the window sizes are bigger, the landmines sizes after mapping are bigger too, and that makes separation for landmines hardly. So, the EF window sizes which we choose are 25.

5. EXPERIMENTAL RESULTS

In this section, we used the proposed approach to detect landmines in the data collected by AMUSAR [20]. The AMUSAR system has been developed since 2010 in China. It operates at stand-off distances, and forms a large area image. Both the range and azimuth resolutions of image are less than 0.2 m. Fig. 5 gives a picture of the AMUSAR system.

As shown in Fig. 6, results using the proposed approach are given. After MCACC, the Fig. 4(c) can be decomposed into three parts: Fig. 6(a) is the curvelet component; Fig. 6(b) is DCT component; and Fig. 6(c) is residual component. The curvelet component mainly contains clutters, while the residual component is made up of noise. Fig. 6(b) mainly contains the landmines. Fig. 6(d) is the detection image using algorithm proposed in this paper, which is DCT component via CFAR detector. After detection, the pixels below the threshold are set to be zeros, and the others will be preserved. In Fig. 6(d), all landmines in this sense are detected with few false alarms in the image.

In order to analyze the performance of each step in Fig. 3, Fig. 7 shows the detection images via CFAR detector for both the TV denoising image and the EF mapping image. There are many false alarms in detection images. For acquiring more accurate conclusion, the receiver operator characteristic (ROC) curves are adopted [23].

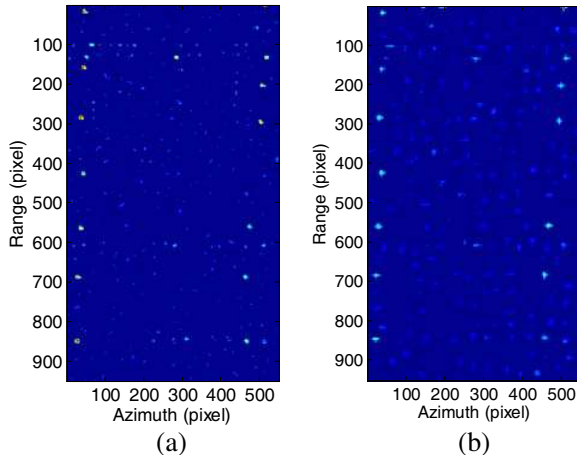


Figure 7. The detection results when the parameter of false alarms rate in CFAR detector is 10^{-3} . (a) The Detection result of image after TV denoising; (b) the detection result of image after EF mapping.

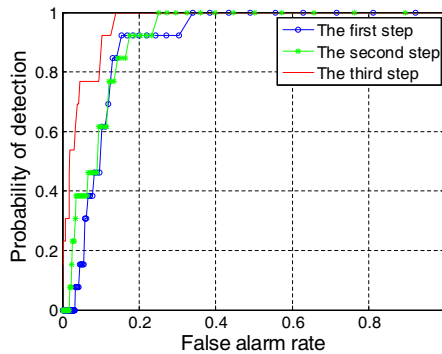


Figure 8. ROC curves for each step in Fig. 3.

Fig. 8 gives the ROC curves for each step in dealing process. As it was expected, since all steps in this paper are executed, the third step can produce the best of the results.

6. CONCLUSION

In this paper, the key is focused on providing a robust and reliable method for minefield detection in a noisy background. A novel approach based on morphological diversity is proposed which contains four main steps. Firstly, TV algorithm is used to suppress the speckle, and it preserves the targets edges well when the number of iteration is 20. Secondly, the parameters values of extended fractal algorithm are selected for acquiring the optimum mapping, after which the spot is well sparse in DCT dictionary. Thirdly, the MCACC algorithm which is a modification of MCA has been designed to separate landmines from image. Through these processing, at last, landmines are detected via DCT component simultaneously with the increasing SCR. The performance of the proposed approach is illustrated using the data acquired over a real airship mounted SAR system

ACKNOWLEDGMENT

This work was supported by the National Natural Science Foundation of China under Grants 60972121, 61271441, and 61201329; the Foundation for the Author of National Excellent Doctoral Dissertation of China under Grant 201046; the Program for New Century Excellent Talents in University under Grant NCET-10-0895; the research project of NUDT under Grant CJ12-04-02.

REFERENCES

1. Mohammadpoor, M., R. S. A. Raja Abdullah, A. Ismail, and A. F. Abas, "A circular synthetic aperture radar for on-the-ground object detection," *Progress In Electromagnetics Research*, Vol. 122, 269–292, 2012.
2. Jin, T., J. Lou, and Z. M. Zhou, "Extraction of landmine features using a forward-looking ground penetrating radar with MIMO array," *IEEE Transactions on Geoscience and Remote Sensing*, Vol. 50, No. 10, 4135–4144, 2012.
3. Moussally, G., R. Fries, and R. Bortins, "Ground-penetrating synthetic-aperture radar for wide-area airborne minefield detection," *Proc. of SPIE*, 1042–1052, 2004.
4. Wang, Y. M., Q. Song, T. Jin, Y. Shi, and X.-T. Huang, "Sparse time-frequency representation based feature extraction method for landmine discrimination," *Progress In Electromagnetics Research*, Vol. 133, 459–475, 2013.
5. Habib, M. A., et al., "Ca-CFAR detection performance of radar targets embedded in 'non centered Chi-2 Gamma' clutter," *Progress In Electromagnetics Research*, Vol. 88, 135–148, 2008.
6. Kwon, H. and N. M. Nasrabadi, "Kernel RX-algorithm: A nonlinear anomaly detector for hyperspectral imagery," *IEEE Transactions on Geoscience and Remote Sensing*, Vol. 43, No. 2, 388–397, 2005.
7. Chen, J., J. Gao, Y. Zhu, W. Yang, and P. Wang, "A novel image formation algorithm for high-resolution wide-swath spaceborne SAR using compressed sensing on azimuth displacement phase center antenna," *Progress In Electromagnetics Research*, Vol. 125, 527–543, 2012.
8. Starck, J.-L., M. Elad, and D. Donoho, "Image decomposition via the combination of sparse representation and a variational approach," *IEEE Transactions on Image Processing*, Vol. 14, No. 10, 1570–1582, 2005.
9. Bobin, J., et al., "Sparsity and morphological diversity in blind source separation," *IEEE Transactions on Image Processing*, Vol. 16, No. 11, 2662–2674, 2007.
10. Huang, C.-W. and K.-C. Lee, "Application of ICA technique to PCA based radar target recognition," *Progress In Electromagnetics Research*, Vol. 105, 157–170, 2010.
11. Candes, E. J., et al., "Fast discrete curvelet transforms," *Applied and Computational Mathematics*, Vol. 91125, 1–43, Caltech, Pasadena, CA, 2005.

12. Ahmed, N., T. Natarajan, and K. R. Rao, "Discrete cosine transform," *IEEE Transactions on Computers*, 90–93, 1974.
13. Kaplan, L. M., "Improved SAR target detection via extended fractal features," *IEEE Transactions on Aerospace and Electronic Systems*, Vol. 37, No. 2, 436–451, 2001.
14. Kaplan, L. M., R. Murenzi, and K. Namuduri, "Extended fractal feature for first stage SAR target detection," *Proc. of SPIE*, Vol. 3721, 35–46, 1999.
15. Rudin, L. I., S. Osher, and E. Fatemi, "Nonlinear total variation based noise removal algorithms," *Physica D: Nonlinear Phenomena*, Vol. 60, 259–268, 1992.
16. Chan, T. F. and S. Esedoglu, "Aspects of total variation regularized L_1 function approximation," *UCLA CAM Report*, 04–07, 2004.
17. Lee, J. S., "Digital image enhancement and noise filtering by use of local statistics," *IEEE Transactions on Pattern Analysis Machine Intelligence*, 165–168, 1980.
18. Kuan, D. T., et al., "Adaptive noise smoothing filter for images with signal-dependent noise," *IEEE Transactions on Pattern Analysis Machine Intelligence*, 165–177, 1985.
19. Cheng, J., G. Gao, W. Ding, X. Ku, and J. Sun, "An improved scheme for parameter estimation of G^0 distribution model in high-resolution SAR images," *Progress In Electromagnetics Research*, Vol. 134, 23–46, 2013.
20. Song, Q., et al., "Results from an airship-mounted ultra-wideband synthetic aperture radar for penetrating surveillance," *Asia-Pacific Conference on Synthetic Aperture Radar*, 194–197, Seoul, Korea, 2011.
21. Wei, S.-J., X.-L. Zhang, J. Shi, and G. Xiang, "Sparse reconstruction for SAR imaging based on compressed sensing," *Progress In Electromagnetics Research*, Vol. 109, 63–81, 2010.
22. Candes, E. J., J. Romberg, and T. Tao, "Robust uncertainty principles: Extract signal reconstruction from highly incomplete frequency information," *IEEE Trans. Inf. Theory*, Vol. 52, 489–509, 2006.
23. Makal, S., A. Kizilay, and L. Durak, "On the target classification through wavelet-compressed scattered ultrawide-band electric field data and ROC analysis," *Progress In Electromagnetics Research*, Vol. 82, 419–431, 2008.